Australian Earthquake Engineering Society
2022 National Conference, 24-25 November 2022
Mount Macedon, Victoria, Australia

Fibre-optic sensors in reinforced concrete walls: a comparison of core to surface strain measurements

Ryan D Hoult[1], Alex Bertholet[1], and João Pacheco de Almeida[1]

1. Institute of Mechanics, Materials and Civil Engineering, UCLouvain, Louvain-la-Neuve, Belgium.

Abstract

High resolution, distributed reinforcement strain measurements can provide invaluable information for developing and evaluating numerical and analytical models of reinforced concrete structures. A recent testing campaign in the Institute of Mechanics, Materials and Civil Engineering (iMMC) at the Université catholique de Louvain (UCLouvain), Belgium, used fibre optic sensors along several longitudinal reinforcement of three reinforced concrete U-shaped walls. To the knowledge of the authors, this is the first example where distributed fibre optic sensors have been used to measure the strain profiles of longitudinal reinforcing bars in structural walls and to such a high spatial resolution. This paper presents some of the preliminary results from the three tested wall units, which include strains both in compression and tension. The latter measurements are compared to other more common instrumentation used in the tests, including those attained from digital image correlation techniques. This state-of-the-art measurement technique has the potential to solve many long-standing questions on reinforced concrete member response and quantifying the phenomena that are currently only known qualitatively.

Keywords: fiber; optical; RC; core walls; C-shaped; plasticity; cracking; yield penetration; DIC

1 Introduction

The ability to measure the entire reinforcement strain profile within reinforced concrete (RC) structures has the potential to help solving many long-standing questions on the mechanisms involved in their response and quantify different phenomena that are currently only known qualitatively. Until recently, many “spot sensors”, such as strain gauges, were required to be used along the length of the rebar to approximately derive strain profiles, a time consuming and costly exercise; take the experimental study investigating tension stiffening effects by Scott and Gill (1987), for example, where 84 strain gauges were installed within a single longitudinal reinforcing bar, or the pioneering and well-know investigations by Shima *et al.* (1987) for the development of local bond stress-slip-strain relations, where relatively dense meshes of strain gauges were also employed. Strain gauges also impose other limitations, including an alteration of the characteristic behaviour of the reinforcing steel, as well as affecting the bond performance to the surrounding concrete (Mata-Falcón *et al.*, 2020). Alternatively, meshes of light-emitting diodes (LEDs) for camera tracking have also been glued at regular spacing to steel rebars visible through concrete voids created during the casting phase (Tarquini *et al.*, 2019). Recent technological improvements to Distributed Fibre Optic Sensors (DFOS) have the potential to measure the full strain profile of steel reinforcement embedded in concrete structures. When the fibres, acting as the sensor, are subjected to an extension or contraction, the frequency of the backscattered light is altered due to the change in distance between the imperfections caused in the cylindrical geometry of the fibres (Malek *et al.*, 2019). A measurement system, known as an interrogator, is then able to analyse the characteristics of the backscattered light and provide strain data. A more complete and detailed explanation of this process can be found in the literature (Bado & Casas, 2021; Zhang *et al.*, 2022). Some of the unique features of DFOS include, but are not limited to, its high accuracy (e.g., ±25 με for a pitch of 0.65mm), repeatability, stability, resistance to electromagnetic interference, protection from corrosion, light mass, small size (e.g., diameter of 125 μm), and low cost (Malek *et al.*, 2019).

Despite recent advances in the last decade, the application of DFOS in RC structures is still in its infancy (Zhang *et al.*, 2022). However, there has been some recent research using DFOS embedded in RC structures (Malek *et al.*, 2019; Zdanowicz *et al.*, 2022; Zhang *et al.*, 2022). To the authors knowledge, only one experimental investigation used DFOS in RC walls. In the study by Woods *et al.* (2017), DFOS was bonded to the surface of the outermost layer of carbon fiber reinforced polymer to measure the strain distribution over the entire face of the strengthened RC wall. No experimental investigation using DFOS bonded to the longitudinal reinforcing steel in RC walls has been found by the authors in the literature.

In this paper, a summary is provided of a recently completed experimental campaign the Université catholique de Louvain (UCLouvain), Belgium, in the technological platform LEMSC (Laboratoire Essais Mécaniques, Structures et Génie Civil) of the Institute of Mechanics, Materials and Civil Engineering (iMMC). The experimental program involved testing three large-scale RC U-shaped walls subjected to different combinations of flexure and torsion. State-of-the-art technology, based on the DFOS system, was used to capture the strain profiles along the entire length of several longitudinal reinforcing bars in each wall unit. The authors will herein present some of the experimental observations obtained thus far in the ongoing data-analysis phase, with a direct comparison of the strains from the DFOS system to those determined from the 3-dimensional displacement field of the surface captured by digital image correlation (DIC) techniques. The authors are currently preparing to submit a manuscript that will provide a more extensive set of experimental results and findings, including additional comparisons with micrometres and linear variable differential transformers (LVDTs). For the sake of brevity, in this conference paper, only the results from one of the three wall units will be presented. More detailed information about the specifics of the tests, as well as the experimental observations, can be found in a recently submitted Data Paper (Hoult *et al.*, 2022). A general summary of the experimental program and some of the instrumentation used is given in the next section.

2 Summary of Experimental Program and Instrumentation

One of the three wall units in the test programme is presented in this paper: wall unit UW1 is a half-scale specimen of a 6-story prototype core wall. The test specimen corresponded to approximately 1.4 stories, where an overturning moment was applied to the collar (i.e., head) of the test specimen to increase the shear span to one characteristic of a 6-storey building. All of these U-shaped wall test specimens have a thickness (t_w) of 100 mm, web length (L_w) of 1300 mm, and flange length (L_f) of 1050 mm. The geometry with reinforcement detailing is illustrated in Figure 1a, and the elevation view of the test specimen is given in Figure 1b.

Ductile Class C reinforcing steel was used for the longitudinal and transverse reinforcement in the wall in accordance with Eurocode 8 (CEN, 2004). The corresponding mechanical properties of the rebars used in the wall units are given in Table 1.

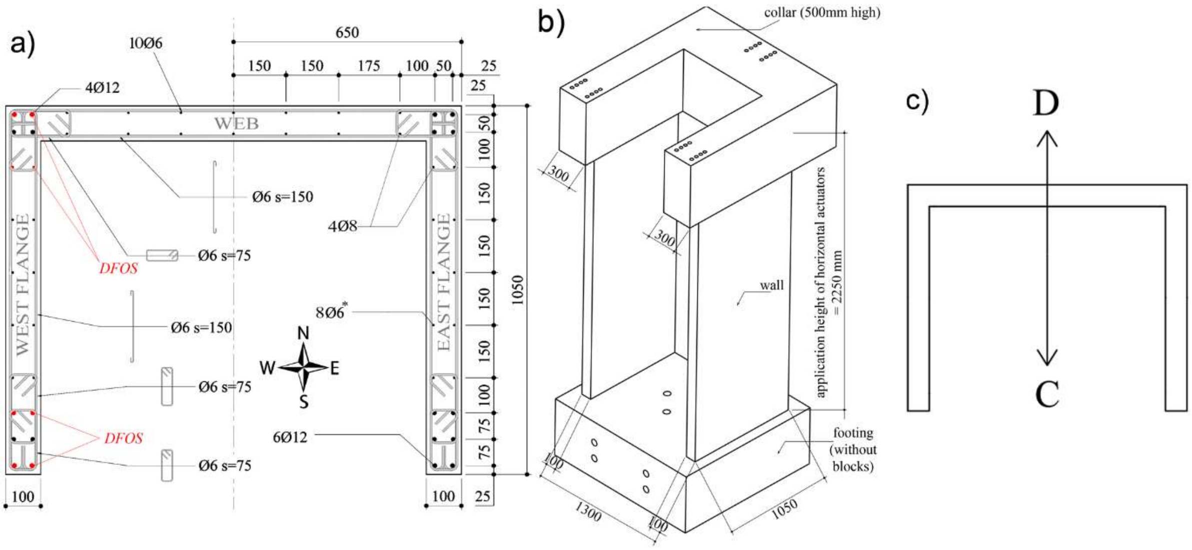

Figure 1. (a) Cross-section and reinforcement detailing of the wall specimens, (b) elevation view, and (c) loading positions of the wall

Table 1. Mechanical properties of the Class C (CEN, 2004) bars used in the wall units

d_{bl}	f_y	f_u	ε_{sy}	ε_{su}	E_s
[mm]	[MPa]	[MPa]	[mm/m]	[mm/m]	[GPa]
6	550	676	2.7	9.5	207
8	538	664	2.7	12.0	196
12	580	690	2.9	10.1	199

Specimen UW1 was loaded parallel to the flanges to positions C and D (Figure 1c), corresponding to the wall bending about the minor axis (i.e., parallel to the flanges) with web in tension and web in compression, respectively. A constant axial load ratio (*ALR*) of 5% was subjected prior to the flexural or torsional loading. An overturning moment was also applied to the wall with vertical actuators, which increased its shear span to approximately 6.72m. More details are discussed in Hoult et al. (2022), currently under review.

For the sake of brevity, the focus of the discussion on the instrumentation will be limited to the information needed for the results provided in this brief paper. The DFOS was implemented using the ODiSI 6000 Series sensing platform (Luna Innovation Inc). Four fibre-optics were attached to a total of eight longitudinal reinforcing bars in each wall unit to investigate the strain profile in the core of the wall. For this paper, the focus is on the strain measurements from the DFOS system located in the *boundary region of the intersection of the web and the West flange*, as indicated in Figure 2 (i.e., an idealized boundary column). A polyimide coated, single-mode sensing fibre type was used. A small groove (i.e., slit of 1 mm width and depth) was cut along the longitudinal ribs of the rebar, which has been widely practiced in previous research for attaching the DFOS to steel reinforcement and to help prevent a premature failure of the fibre (Bado *et al.*, 2020; Michou *et al.*, 2015; Quiertant *et al.*, 2012; Zdanowicz *et al.*, 2022; Zhang *et al.*, 2021). A general-purpose adhesive (cyanoacrylate) was used to bond the fibre into the grove of the bar, which has also been successfully used in the literature for this purpose (Barrias *et al.*, 2018; Berrocal *et al.*, 2021; Brault & Hoult, 2019; Zdanowicz *et al.*, 2022). An epoxy was also used to provide a coating of further protection between the glued-fibre and the concrete. To compare with the DFOS measurements, the 3-dimensional displacement field of the web captured using DIC techniques is employed. A speckle pattern for the DIC measurements was applied on two outside surfaces of the wall units (East flange and web) covering the full height of the wall units from the base to a height of 2 meters. The speckle pattern was applied by a stencil to produce a random pattern of black dots with an approximate diameter of 2−3 mm. Two three-dimensional DIC systems were used, i.e. two sets of two high resolution (12 megapixel) cameras recorded monochrome (i.e., black and white) images at a frequency of 0.2 Hz (i.e., every 5 s) during testing. The images were processed using a program called Istra4D, where the displacement and strain field was exported into tab-separated values to be further processed and analysed in MATLAB (Mathworks, 2020).

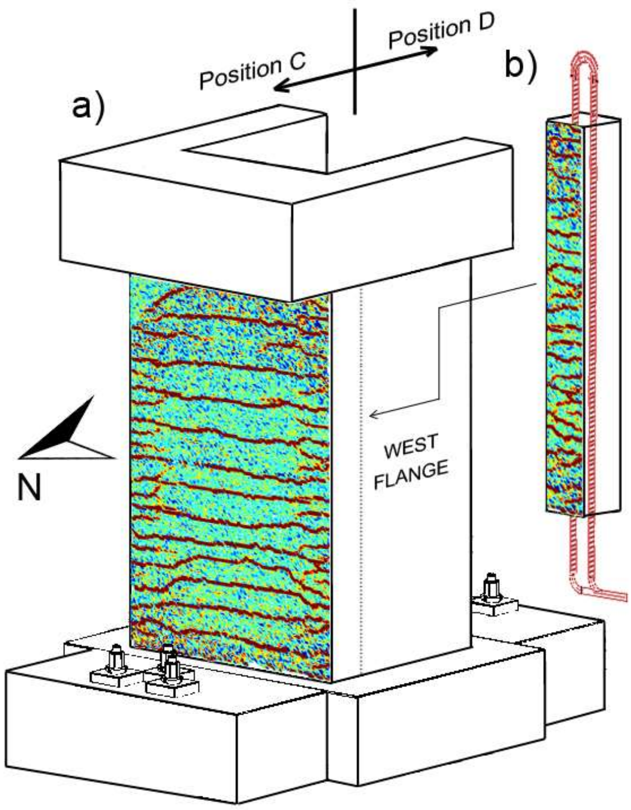

Figure 2. (a) 3-dimensional illustration of the RC U-shaped wall unit with foundation blocks and DIC strain results on the surface of the web (b) column of the West flange-web intersection (100 x 100 mm² cross-section) with DIC surface and embedded DOFS sensors

3 Surface versus core strain estimates

For these comparisons, strain measurements will be investigated for load stages where the web-flange intersection is either in tension or in compression, which corresponds to the first wall unit (UW1) pushed and pulled to positions C and D (Figure 1c), respectively.

Figure 3 and Figure 4 plot the measured strains from the DIC and DFOS systems at position C (tension) and position D (compression), respectively, and for drift (δ) levels of 0.2%, 0.4%, and 0.6%. The thin-blue lines plot the "raw" strains determined from the DIC, with a discrete gauge distance in the vertical direction of just 8.5 mm. In comparison to the DFOS-measured strains, which are plotted as thick-black lines, a scatter of results can be observed from the DIC, with large tensile and compressive peaks. This feature has been observed in other research on RC walls using DIC strain measurements with small gauge lengths (e.g., Hoult & Beyer, 2021). This can be expected and explained to a certain extent, since the tensile strains, for example, are calculated over a very small base length, where the small changes in vertical deformations, typically occurring at crack locations, result in peak, concentrated strain values. In the case that the DIC data is of high-resolution, it is likely that this data will need to be averaged over a certain base length to provide more reasonable values. In Hoult and Beyer (2021), the DIC strains were averaged over a length of 100mm, equal to the thickness of the wall, a choice made at the time due to lack of guidance provided elsewhere. Instead, the authors here argue that the DIC strains could be averaged over a length which is equal to the spacing of the transverse reinforcement. For example, notice in Figure 3 that each of the peaks of tensile strain determined by the "uncorrected" (i.e., high-resolution, small base length) DIC data occurs at approximately every 75mm. This length is equal to the spacing of the transverse ties detailed in this corner of the wall. As the distributed, flexural cracks up the height of the wall are highly influenced by the placement of the transverse steel (i.e., confinement or shear reinforcement), it can be assumed as rough guess that these peak tensile strains captured by the DIC occur approximately at the locations of these steel rebars. Alternatively, more accurate estimates of the crack spacing can be used. Thus, the uncorrected DIC strains have been averaged over a length of 75mm, which is the spacing of the transverse confinement of the wall, and plotted in Figure 3 and Figure 4 (thick-red lines). As observed in these figures, a better match, particularly in terms of global trend – and less so in terms of smoothness, between the DFOS-measured strains and the average calculated DIC strains, is achieved, particularly for the tensile strains given in Figure 3. It is worth mentioning that, while the results shown here are encouraging, this only represents the preliminary stages of the analyses conducted by the authors, and further conclusions are expected to be presented in a future journal paper.

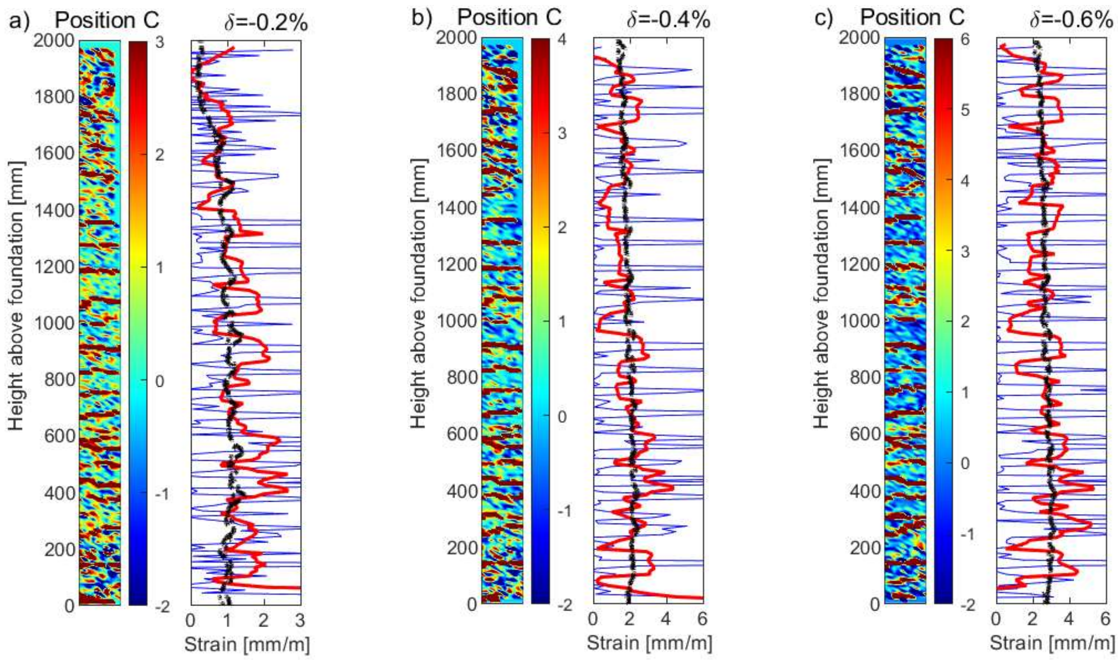

Figure 3. Strain measurements in UW1 at position C (i.e., web in tension) using different technology at drift levels: (a) δ=-0.2%, (a) δ=-0.4%, (a) δ=-0.6%. Thin blue lines are the uncorrected (raw), discrete strains from DIC, thick red line is the corrected (i.e., averaged over 75mm) strains from DIC. The black, dashed line indicates the high-resolution strains measured from the DFOS.

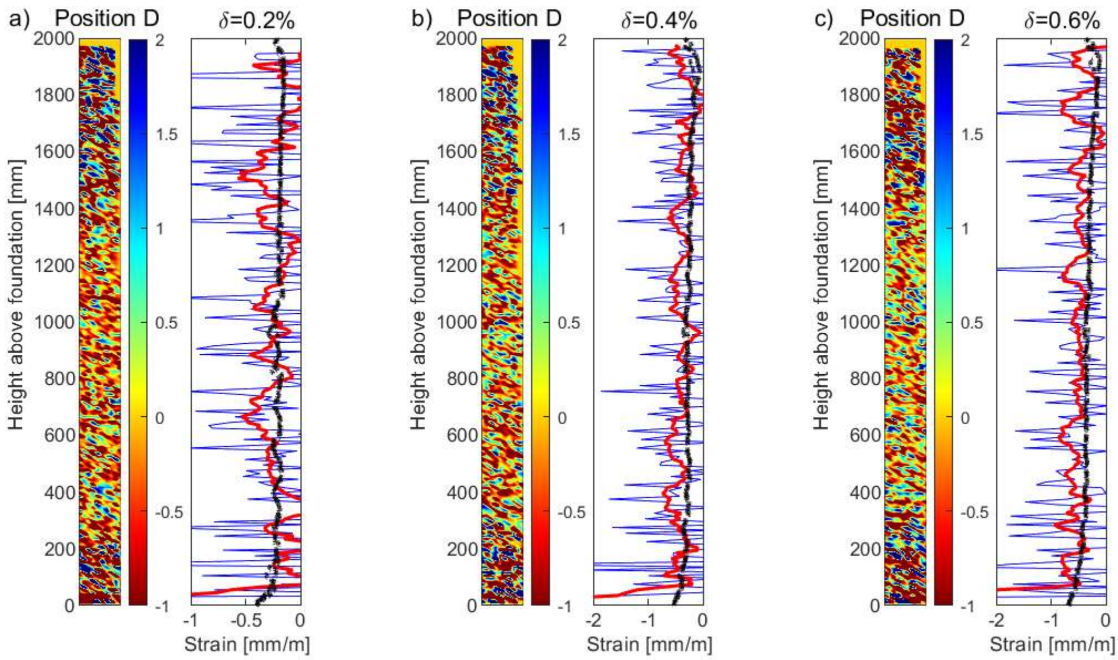

Figure 4. Strain measurements in UW1 at position D (i.e., web in compression) using different technology at drift levels: (a) δ=0.2%, (a) δ=0.4%, (a) δ=0.6%. Thin blue lines are the uncorrected (raw), discrete strains from DIC, thick red line is the corrected (i.e., averaged over 75mm) strains from DIC. The black, dashed line indicates the high-resolution strains measured from the DFOS.

4 Conclusions

The longitudinal strains measured on the surface and along longitudinal rebars in the core of a RC U-shaped wall were investigated in this paper. DFOS can provide high-resolution, high-accuracy strain values with very limited calibration required. However, a major limitation of this technology appears to be a limiting strain of approximately 1%, which is a problem for RC structures that get pushed into the inelastic range. On the other hand, the calibration required for DIC surface strain measurements can be quite time consuming and dependent on many factors (e.g., lighting). Whilst typically less accurate than the DFOS measurements, DIC surface strain measurements can be obtained throughout the testing of large-scale RC structures, up until major damage has accumulated (e.g., spalling of the concrete surface, crushing of the concrete, etc). Thus, these two instrumentation methods have many advantages, as well as some disadvantages. However, the use of both technologies for data acquisition of large-scale tests, such as that presented here, can be hugely advantageous in providing detailed analyses of these structures.

It was shown in this research that the DIC surface strain measurements compared reasonably well to the strains measured internally using DFOS along the length of the rebars. However, it was shown that, when measuring high-resolution strains with DIC techniques, the resulting values need to be averaged over a reasonable and rational base length. While this is not necessarily a new observation, there appears to be no guidance for what base length should be used. In this paper, the authors tentatively suggest a simple and quick-to-use gauge (or base) length equivalent to the spacing of the transverse confinement reinforcement. In the absence of confinement, a base length equivalent to the spacing of the transverse shear reinforcement could be used. This is due to the DIC tensile strain measurements typically corresponding to peak strains located at cracks, and flexural cracks of RC walls often occur at the placement of the transverse steel. A more thorough investigation is currently being undertaken by the authors, using a greater set of strain data corresponding to other drift levels and also two more wall units. More recommendations will be provided in coming publications, which will help future research using DIC or DFOS measurements for RC structures. These recommendations have the potential to increase the accuracy of future engineering parameters being measured with these systems, such as the strains herein investigated, and hence provide calibration/validation data for model and simulation advancement.

5 Acknowledgements

This work was supported by the Fonds de la Recherche Scientifique – FNRS under Grant nº F.4501.21.

6 References

Bado, M. F., & Casas, J. R. (2021). A Review of Recent Distributed Optical Fiber Sensors Applications for Civil Engineering Structural Health Monitoring. *Sensors, 21*(5). doi:10.3390/s21051818

Bado, M. F., Casas, J. R., Dey, A., & Berrocal, C. G. (2020). Distributed Optical Fiber Sensing Bonding Techniques Performance for Embedment inside Reinforced Concrete Structures. *Sensors, 20*(20), 5788. doi:10.3390/s20205788

Barrias, A., Casas, J. R., & Villalba, S. (2018). Embedded Distributed Optical Fiber Sensors in Reinforced Concrete Structures—A Case Study. *Sensors, 18*(4), 980. doi:10.3390/s18040980

Berrocal, C. G., Fernandez, I., & Rempling, R. (2021). Crack monitoring in reinforced concrete beams by distributed optical fiber sensors. *Structure and Infrastructure Engineering, 17*(1), 124-139. doi:10.1080/15732479.2020.1731558

Brault, A., & Hoult, N., A. (2019). Distributed Reinforcement Strains: Measurement and Application. *ACI Structural Journal, 116*(4). doi:10.14359/51714483

CEN. (2004). Eurocode 8: Design of structures for earthquake resistance. Part 1, EN 1998-1. In.

Hoult, R., & Beyer, K. (2021). RC U-shaped walls subjected to in-plane, diagonal, and torsional loading: New experimental findings. *Engineering Structures, 233*. doi:10.1016/j.engstruct.2021.111873

Hoult, R., Doneux, C., & João Saraiva Esteves Pacheco De, A. (2022). Tests on Reinforced Concrete U-shaped Walls Subjected to Torsion and Flexure. *Submitted to Earthquake Spectra*.

Malek, A., Scott, A., Pampanin, S., & Hoult, N. A. (2019). Postyield Bond Deterioration and Damage Assessment of RC Beams Using Distributed Fiber-Optic Strain Sensing System. *Journal of Structural Engineering, 145*(4), 04019007. doi:10.1061/(ASCE)ST.1943-541X.0002286

Mata-Falcón, J., Haefliger, S., Lee, M., Galkovski, T., & Gehri, N. (2020). Combined application of distributed fibre optical and digital image correlation measurements to structural concrete experiments. *Engineering Structures, 225*. doi:10.1016/j.engstruct.2020.111309

Mathworks. (2020). MATLAB R2020a Update 3 (9.8.0.1396136).

Michou, A., Hilaire, A., Benboudjema, F., Nahas, G., Wyniecki, P., & Berthaud, Y. (2015). Reinforcement–concrete bond behavior: Experimentation in drying conditions and meso-scale modeling. *Engineering Structures, 101*, 570-582. doi:10.1016/j.engstruct.2015.07.028

Quiertant, M., Baby, F., Khadour, A., Marchand, P., Rivillon, P., Billo, J., . . . Cordier, J. (2012, May 22-24). *Deformation monitoring of reinforcement bars with a distributed fiber optic sensor for the SHM of reinforced concrete structures.* Paper presented at the 9th

International Conference on NDE in Relation to Structural Integrity for Nuclear and Pressurized Components, Seattle, Washington, USA.

Scott, R., & Gill, P. A. (1987). Short-term distributions of strain and bond stress along tension reinforcement. *The Structural Engineer, 65*(2), 39-43.

Shima, H., Chou, L.-L., & Okamura, H. (1987). Micro and macro models for bond in reinforced concrete. *Journal of the Faculty of Engineering, 39*(2), 133-194.

Tarquini, D., Almeida, J. P., & Beyer, K. (2019). Uniaxial Cyclic Tests on Reinforced Concrete Members with Lap Splices. *Earthquake Spectra, 35*(2), 1023-1043. doi:10.1193/041418eqs091dp

Woods, J. E., Lau, D. T., Bao, X., & Li, W. (2017). Measuring strain fields in FRP strengthened RC shear walls using a distributed fiber optic sensor. *Engineering Structures, 152*. doi:10.1016/j.engstruct.2017.09.034

Zdanowicz, K., Gebauer, D., Koschemann, M., Speck, K., Steinbock, O., Beckmann, B., & Marx, S. (2022). Distributed fiber optic sensors for measuring strains of concrete, steel, and textile reinforcement: Possible fields of application. *Structural Concrete*. doi:10.1002/suco.202100689

Zhang, S., Liu, H., Coulibaly, A. A. S., & DeJong, M. (2021). Fiber optic sensing of concrete cracking and rebar deformation using several types of cable. *Structural Control and Health Monitoring, 28*(2), e2664. doi:10.1002/stc.2664

Zhang, S., Liu, H., Darwish, E., Mosalam, K. M., & DeJong, M. J. (2022). Distributed Fiber-Optic Strain Sensing of an Innovative Reinforced Concrete Beam-Column Connection. *Sensors, 22*(10). doi:10.3390/s22103957